Science Advances
AAAS

advances.sciencemag.org/cgi/content/full/5/9/eaax8352/DC1

Supplementary Materials for

Mitochondrial PE potentiates respiratory enzymes to amplify skeletal muscle aerobic capacity

Timothy D. Heden, Jordan M. Johnson, Patrick J. Ferrara, Hiroaki Eshima, Anthony R. P. Verkerke, Edward J. Wentzler, Piyarat Siripoksup, Tara M. Narowski, Chanel B. Coleman, Chien-Te Lin, Terence E. Ryan, Paul T. Reidy, Lisandra E. de Castro Brás, Courtney M. Karner, Charles F. Burant, J. Alan Maschek, James E. Cox, Douglas G. Mashek, Gabrielle Kardon, Sihem Boudina, Tonya N. Zeczycki, Jared Rutter, Saame Raza Shaikh, Jean E. Vance, Micah J. Drummond, P. Darrell Neufer, Katsuhiko Funai*

*Corresponding author. Email: kfunai@utah.edu

Published 11 September 2019, *Sci. Adv.* **5**, eaax8352 (2019)
DOI: 10.1126/sciadv.aax8352

This PDF file includes:

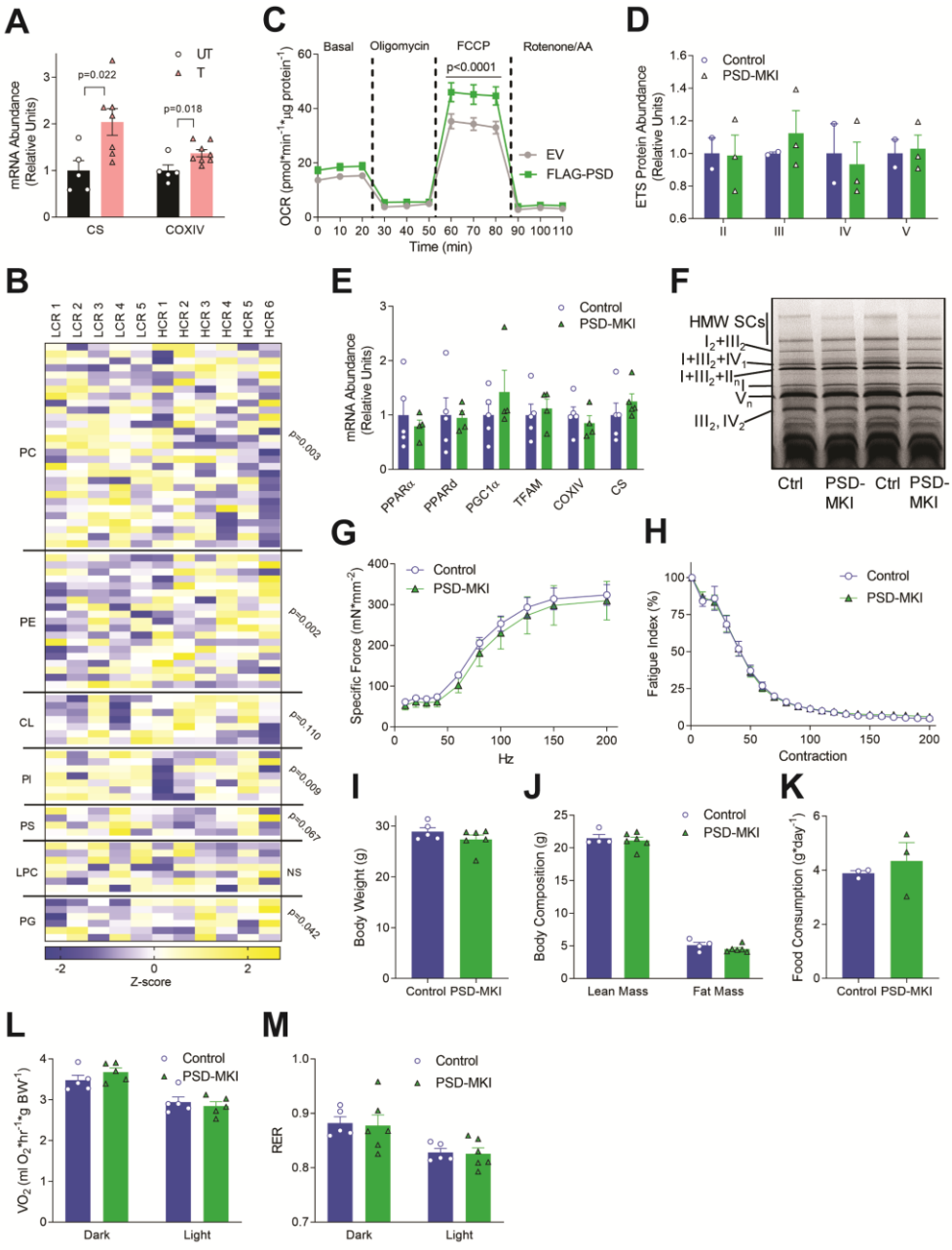

Fig. S1. Skeletal muscle mitochondrial PE and oxidative capacity. (**A**) Skeletal muscle citrate synthase (CS) and cytochrome oxidase IV (COXIV) mRNA in UT or T mice (n=5-8). (**B**) Skeletal muscle mitochondrial phospholipidome in low-capacity running (LCR) or high-capacity running (HCR) rats (n=5-6). (**C**) Oxygen consumption rates (OCR) from empty vector (EV) or PSD-expression vector (FLAG-PSD) treated C2C12 myotubes (n=6). (**D**-**K**) Ctrl or PSD-MKI mice. (D) Quantification of ETS western blot (n=2-3). (E) Muscle mRNA encoding mitochondrial enzymes and transcription factors (n=5). (F) Blue native gel of isolated mitochondria revealing supercomplexes (n=4). High molecular weight supercomplexes (HMW SCs). (G) Force-frequency curve (n=3). (H) Fatigue curve with tetanic contractions (n=5-6). (I) Body weights (n=5-6). (J) Body composition (n=4-6). (K) Food consumption (n=3). (**L**) Whole-body VO_2 (n=5). (**M**) Respiratory exchange ratio (RER, n=5). Mean ±SEM.

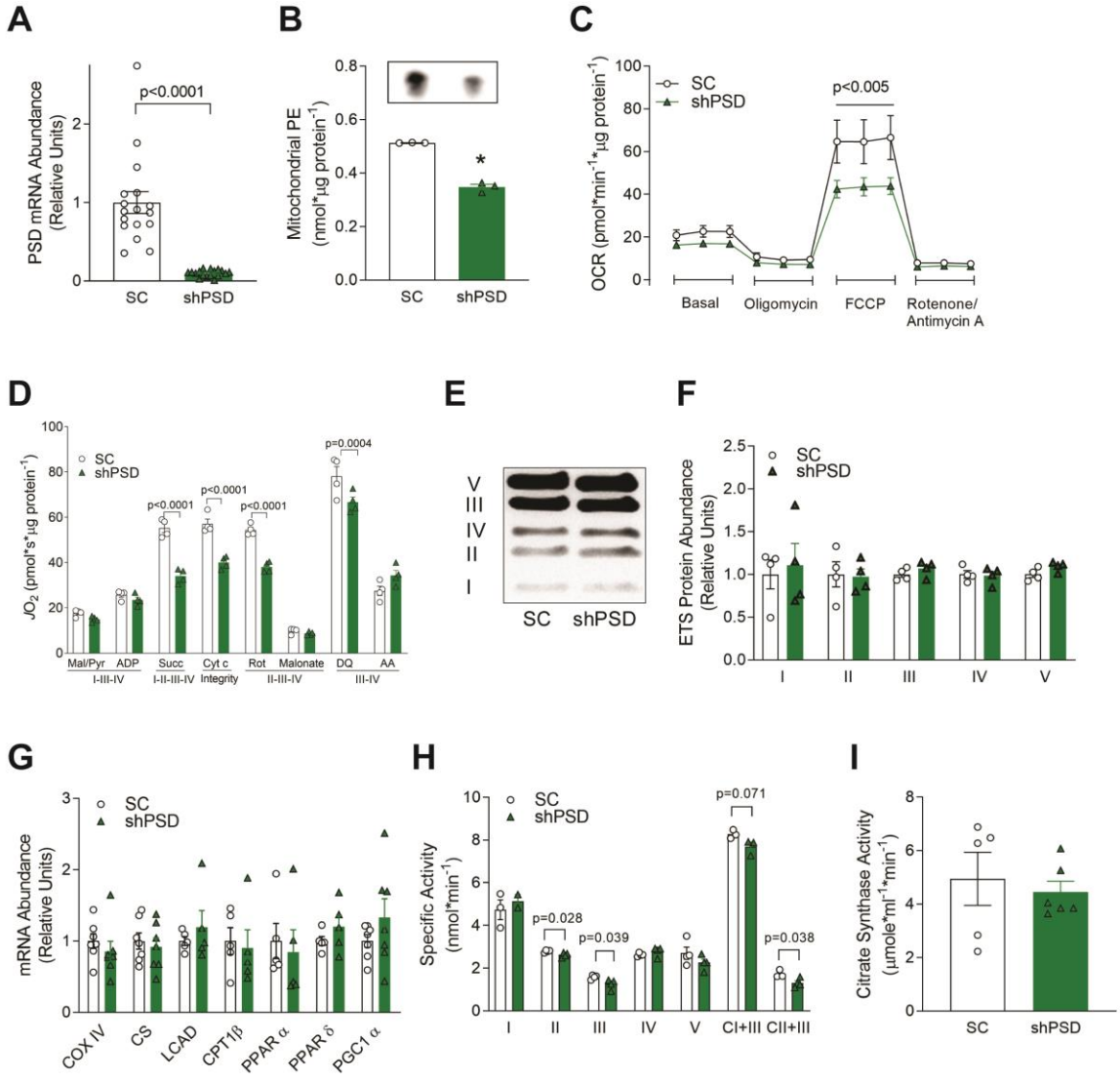

Fig. S2. Deficiency of muscle mitochondrial PE in vitro. (**A-I**) C2C12 myotubes incubated with lentivirus expressing scrambled (SC) or shRNA targeted to PSD (shPSD). (**A**) PSD mRNA (n=17). (B) Mitochondrial PE (n=3). (C) OCR in intact myotubes (n=6). (D) Rate of oxygen consumption using Krebs cycle substrates (n=4). (E) Protein abundance of respiratory complexes I-V. (F) Quantification of respiratory complex proteins (n=4). (G) mRNA encoding mitochondrial enzymes and transcription factors (n=3-4). (H) Activities of respiratory enzymes (n=4). (I) Citrate synthase activity (n=5-6). Mean ±SEM.

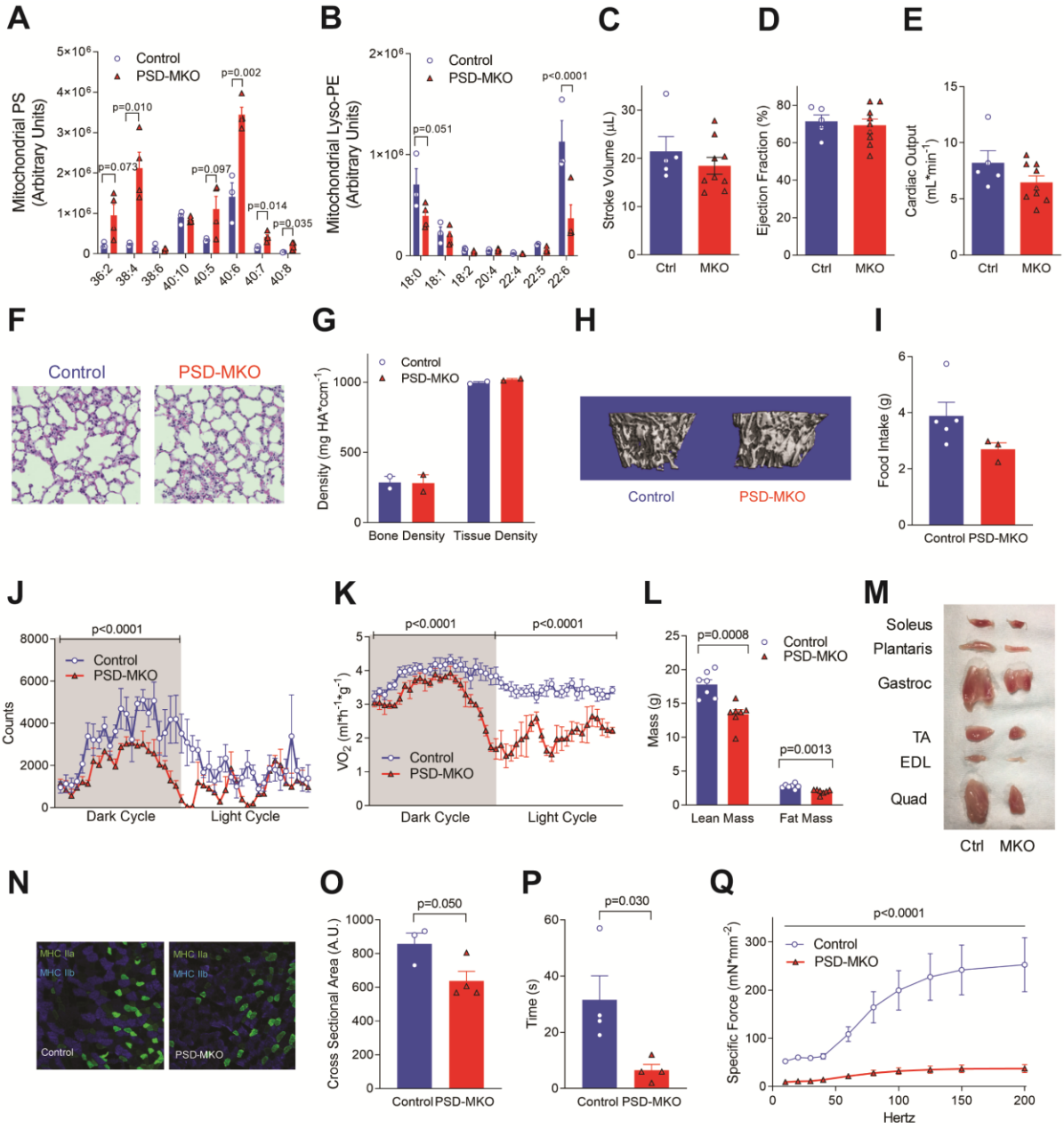

Fig. S3. Deficiency of skeletal muscle mitochondrial PE in vivo. (**A**) Muscle mitochondrial PS (n=3-4). (**B**) Muscle mitochondrial lyso-PE (n=3-4). (**C-E**) Stroke volume, ejection fraction, or cardiac output measured with echocardiography (n=5-8). (**F**) H&E staining of lung section. (**G, H**) Bone density by μCT scan (n=2). (**I**) Food intake (n=3-5). (**J, K**) Activity and VO_2 measured by indirect calorimetry (n=6). (**L**) Body composition (n=7). (**M**) Muscle sizes. (**N**) Fiber-type composition. (**O**) Fiber cross-sectional area (n=3-4). (**P**) Kondziela's inverted screen test (n=4). (**Q**) Force-frequency curve of extensor digitorum longus muscles (n=2-4). Mean ±SEM.

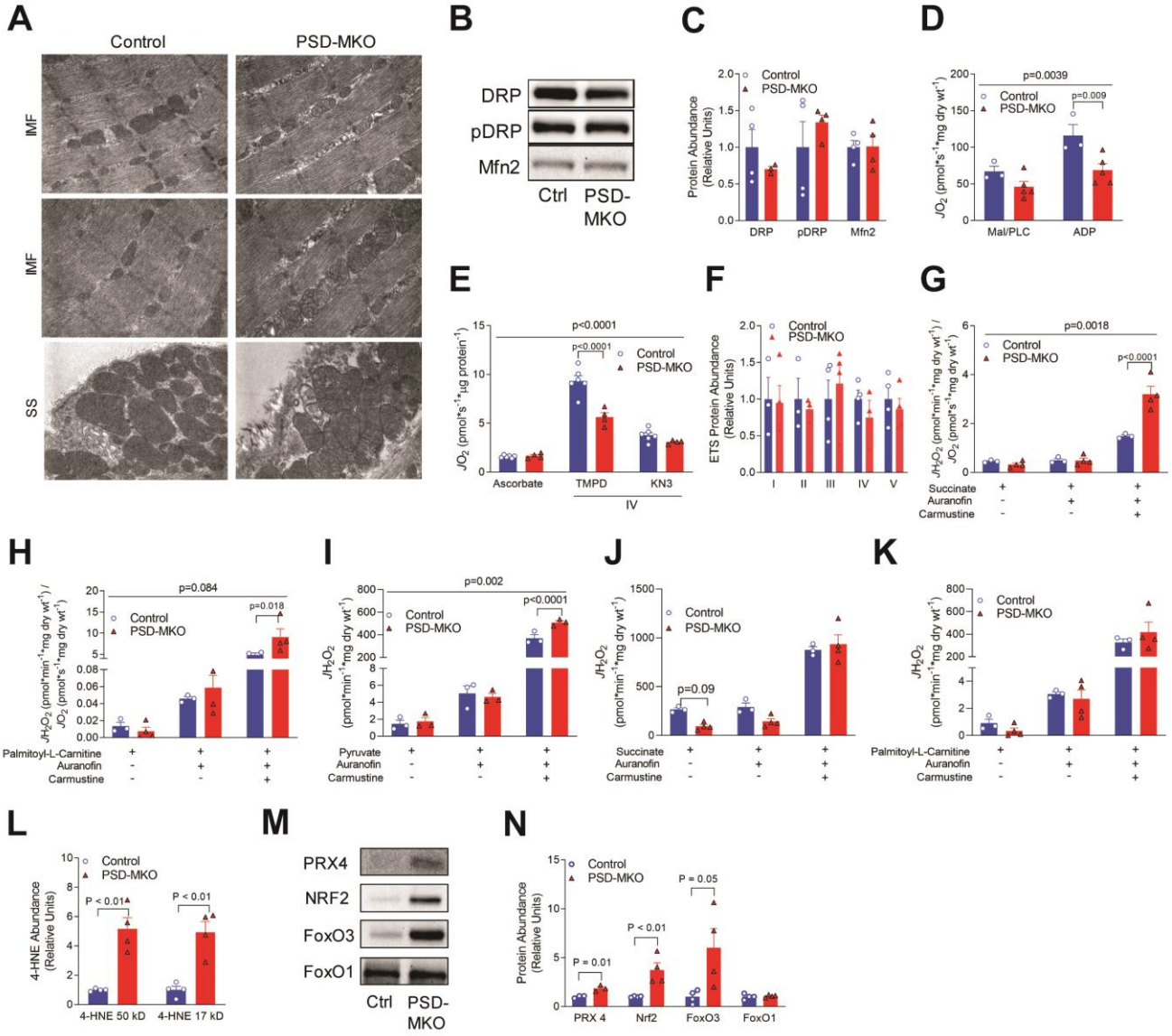

Fig. S4. PE deficiency in skeletal muscle mitochondria. (**A**) EM images of intermyofibrillar (IMF) and subsarcolemmal (SS) mitochondria. (**B**) Total and phosphorylated (Ser 616) dynamin-related protein (DRP) and mitofusion 2. (**C**) Quantification of DRP, pDRP and Mfn2 western blot (n=4). (**D**) Palmitoyl-L-carnitine (PLC)-induced oxygen consumption in permeabilized fibers (n=3-5). (**E**) Complex IV-mediated respiration rates in isolated mitochondria (n=4-6). (**F**) Quantification of ETS protein abundance (n=3-4). (**G**) H_2O_2 production and emission with succinate normalized to O_2 consumption (n=3-4). (**H**) H_2O_2 production and emission with palmitoyl-L-carnitine normalized to O_2 consumption. (**I**) Mitochondrial H_2O_2 production and emission with pyruvate (n=3). (**J**) Mitochondrial H_2O_2 production and emission with succinate (n=3-4). (**K**) H_2O_2 production and emission with palmitoyl-L-carnitine (n=3-4). (**L**) Quantification of 4-HNE western blot (n=3-4). (**M**) Protein abundance of the antioxidant enzyme peroxiredoxin 4 (PRX4) and regulators of antioxidant defense including nuclear factor erythroid 2-related factor 2 (NRF2), forkhead box protein O1 (FoxO1), and FoxO3. (**N**) Quantification of antioxidant defense proteins (n=4). Mean ±SEM.

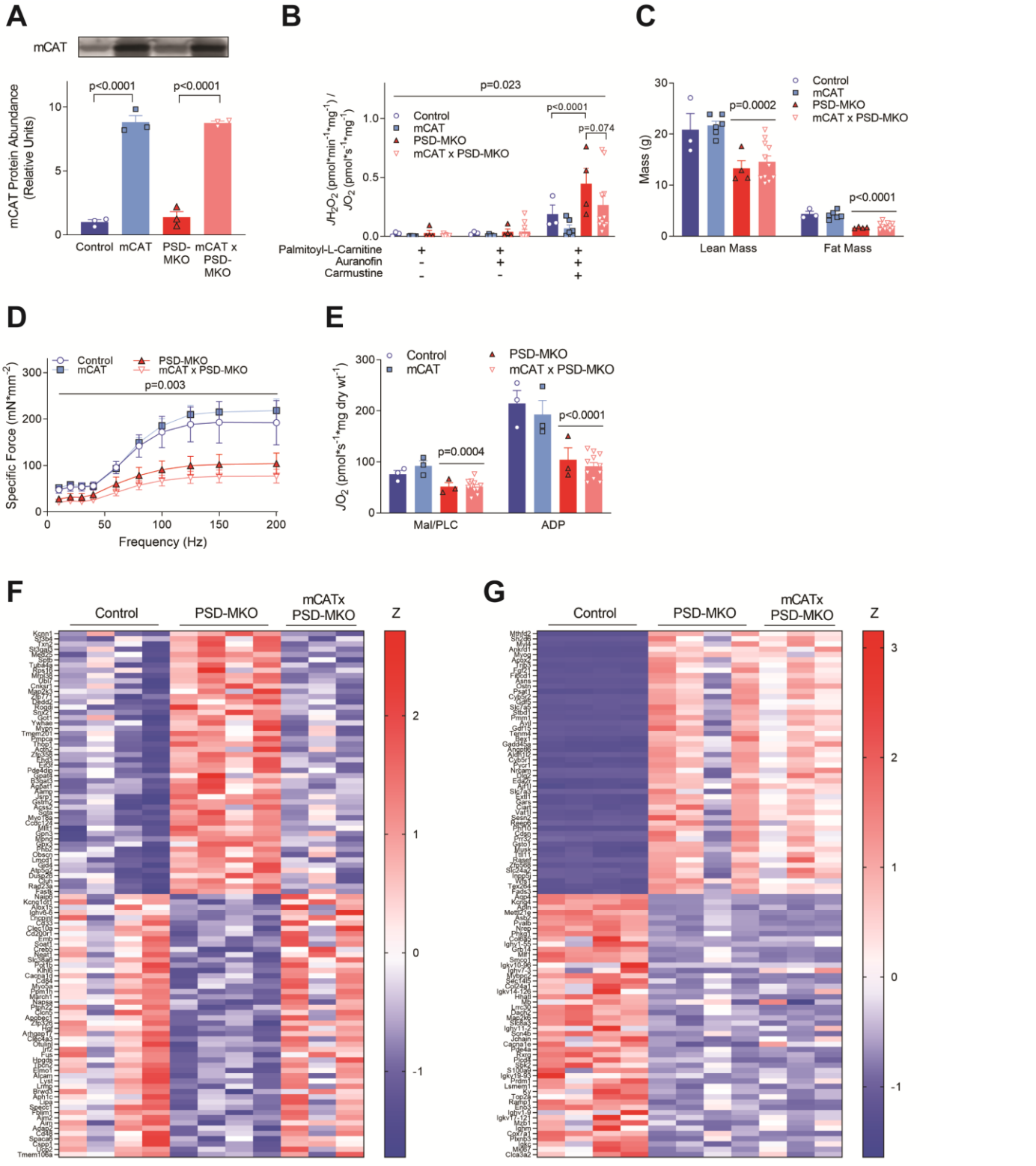

Fig. S5. Overexpression of mitochondrial catalase does not rescue muscle-specific PSD deficiency. (**A**) Protein abundance of mCAT (n=3). (**B**) Mitochondrial H_2O_2 production and emission with palmitoyl-L-carnitine normalized to O_2 consumption (n=3-11). (**C**) Body composition of mice 4-wk post-tamoxifen injection (n=3-11). (**D**) Force frequency curve for extensor digitorum longus (n=3-11). (**E**) Palmitoyl-L-carnitine (PLC)-induced oxygen consumption in permeabilized fibers (n=3-11). (**F**) Heatmap of top 100 (50 high and 50 low) genes that were differentially expressed between control and PSD-MKO diaphragms that were reversed in mCATxPSD-MKO diaphragms. Z: z-score. (n=3-4). (**G**) Heatmap of top 100 (50 high and 50 low) genes that were differentially expressed between control and PSD-MKO diaphragms. Mean ±SEM.